View metadata, citation and similar papers at core.ac.uk
brought to you by CORE
provided by KITopen

Universität Karlsruhe (TH)
Institut für Baustatik

An anisotropic fibre-matrix material model at finite elastic-plastic strains

S. Klinkel, C. Sansour, W. Wagner

Mitteilung 1(2003)

BAUSTATIK

Universität Karlsruhe (TH)
Institut für Baustatik

An anisotropic fibre-matrix material model at finite elastic-plastic strains

S. Klinkel, C. Sansour, W. Wagner

Mitteilung 1(2003)

Prof. Dr.–Ing. W. Wagner
Institut für Baustatik
Universität Karlsruhe
Postfach 6980
76128 Karlsruhe

Telefon: (0721) 608–2280
Telefax: (0721) 608–6015
E–mail: bs@.uni-karlsruhe.de
Internet: http://www.bs.uni-karlsruhe.de

©

Mitteilung IBS 2004; **1**:1–22

An anisotropic fibre-matrix material model at finite elastic-plastic strains

S. Klinkel[1]*, C. Sansour[2], W. Wagner[1]

[1] *Institut für Baustatik, Universität Karlsruhe (TH), 76131 Karlsruhe, Germany*

[2] *School of Petroleum Engineering, University of Adelaide, SA 5005, Australia*

Contents

SUMMARY

In this paper a constitutive model for anisotropic finite strain plasticity, which considers the major effects of the macroscopic behaviour of matrix-fibre materials, is presented. One of the most striking feature of the model is its suitability for a numerical treatment. The matrix material is assumed to be isotropic, the anisotropy is induced by the fibre material. The free energy function is additively split into a part related to the matrix and in parts which correspond to the fibres. The deformation gradient is multiplicatively decomposed into elastic and plastic parts. The principle of the maximum plastic dissipation yields the evolution equations of the plastic variables for matrix and fibres. An implicit integration algorithm for the fibre is proposed, which leads to the classical return-mapping scheme. Some numerical examples demonstrate the anisotropic behaviour of the introduced material model.

KEY WORDS: Anisotropic plasticity, Finite strains, Material modelling, Fibre-Matrix material

1. INTRODUCTION

Anisotropic effects in the elastic-plastic deformation range may occur either due to oriented internal structures, see e.g. [1], or to fibre matrix compositions. The paper is a contribution to analyse fibre-matrix materials using a simple constitutive model which capture the characteristic macroscopic behaviour of the anisotropic material. An accurate modelling is important for the design of materials like e. g. fibrous Boron-Aluminium composites [2] or fibre reinforced composites [3].

The description of anisotropic materials is very often based on averaged quantities. That is, the anisotropic behaviour of the material is captured in an averaged sense. The elasticity

tensor is the most profound example of such description, where two tensorial (second order) quantities are related through an anisotropic fourth order tensor. However, very often tensor-valued relationships can be derived from a scalar function (energy, flow rule), which means that the scalar functions themselves are to be described in an anisotropic manner, that takes possible material symmetries into account. The mathematical means for this is the notion of structural tensors, which is a general tool for describing certain classes of anisotropy and encompasses well established models of elastic anisotropy and anisotropic flow rules, such as the orthotropic yield condition early published in the classical work of Hill [4]. Structural tensors are dyadic products of the privileged directions of the material. Essentially, the anisotropic function under consideration (internal energy, flow rule) is formulated in terms of the so-called integrity basis, which consists of invariants of the main variable (strain or stress) together with invariants of the tensor products of the main variable with the structural tensors. The resulting function is supposed to describe the average behaviour of the system, irrespective of the physical nature of anisotropy itself which may be a result of the crystal structure of the material or a result of the fact that the material is composed of different components such as a matrix and fibres. As examples, anisotropic yield criteria are discussed e.g. in [5], [6], and [7], to mention a few.

Recently a considerable effort has been devoted into the extension of isotropic finite strain models of inelasticity to the anisotropic case. In this regard a clear distinction can be drawn between models based on additive decompositions of suitable strain measures as in [8], [9], or [10], and those which are based on the multiplicative decomposition of the deformation gradient into elastic and inelastic parts such as in [11], [12], [13], or [14]. An important issue in relation to these different models is the effort to be considered with regard to numerical implementations.

In fact, anisotropic schemes based on averaged description are very involved. Of the above mentioned, those based on the multiplicative decomposition lead to especially involved and tedious schemes and the numerical effort to obtain solutions can be very considerable.

This paper is concerned with a simple constitutive model for fibre reinforced material at finite elastic-plastic strains. The material is assumed to consist out of a matrix and one or more fibres. The model is characterized by its conceptual simplicity as well as its numerical efficiency. The numerical effort essentially can be compared with that known from purely isotropic computations. The main idea is to consider the continuum as superimposed of the matrix and further one-dimensional continua each of them represent one family of fibres. The fibres are assumed to be equally distributed over the body. The different continua are linked by the kinematic constraint that the deformation gradient applies to all of them. The elastic-plastic model is based on the multiplicative decomposition of the deformation gradient into an elastic and plastic part, for both the matrix and the fibre. The free energy function is additively decomposed into an isotropic part for the matrix and into parts for the fibres, which induce the anisotropic behaviour.

The greatest advantage of such formulation, as compared to an averaged description, lies in the possibility of treating each constituent separately. While the matrix can be considered isotropic and well established schemes can be applied, a specific formulation must be developed for the one-dimensional continua which are supposed to capture the behaviour of the fibres. In fact, it turns out that a simple formulation can be found rendering the whole approach extremely efficient. The essential features and novel aspects of the presented formulation are summarized as follows:

i) The additive split of the free energy function leads to separated constitutive equations

for the matrix and the fibres. For the matrix we use an isotropic elastic-plastic model for large strains, which was proposed in [15].

ii) For the fibre a one-dimensional material model is introduced. The governing equations are derived with the principle of maximum dissipation and the yield condition as a constraint.

iii) The introduced constitutive model is able to consider various fibres with arbitrary directions. A formulation of an anisotropic yield condition, which captures all material symmetries, is not necessary.

iv) An implicit integration method yields a scalar-valued return mapping algorithm for each fibre, which, along with a consistent tangent modulus, is very efficient for numerical implementation.

v) To obtain quadratic convergence in the frame of the Newton-Raphson method, the consistent elastic-plastic tangent modulus for the fibre is derived. The tangent modulus for the matrix material may be found in [16].

The paper is organized as follows: In Section 2 the anisotropic constitutive model is proposed. First the kinematics of multiplicative elastoplasticity are summarized. The free energy function is introduced. On this basis the elastic and plastic constitutive models are derived along standard arguments in rational continuum mechanics. In Section 3 an implicit integration algorithm for the rate independent plasticity formulation is presented. On this framework the algorithmic elastic-plastic tangent modulus is derived. Finally, numerical examples in Section 4 demonstrate the anisotropic behaviour of the proposed model.

2. ANISOTROPIC CONSTITUTIVE MODEL

2.1. Kinematics

Let the deformation $\phi(\boldsymbol{X},t)$ be a point map form the body $\mathcal{B}$ with $\boldsymbol{X} \in \mathcal{B}$ to the actual configuration $\mathcal{B}_t$ at the time t. The tangent to ϕ is denoted the deformation gradient $\boldsymbol{F}(\boldsymbol{X}) : \boldsymbol{T}\mathcal{B} \rightarrow \boldsymbol{T}\mathcal{B}_t$. If $\boldsymbol{X}$ and $\boldsymbol{x}$ are the co-ordinates of the body $\mathcal{B}$ and the actual configuration $\mathcal{B}_t$, the deformation gradient is given by

$$\boldsymbol{F} = \mathrm{Grad}_X(\boldsymbol{x}) \quad . \tag{1}$$

A fundamental assumption is now that the above kinematics applies to a body which exhibits more then one constituent. The constituents differ not only with respect to their material behaviour but in their geometry as well. In our specific case, we assume that one constituent will always be an isotropic classical continuum. Each of the other constituents will be defined as a continuum which deforms and carries loads only in one specific direction, the direction of a corresponding family of fibres. Of such continua there will be as much as there are families of fibres.

A multiplicative decomposition, which may be motivated by a micro-mechanical view of plastic deformations, into an elastic part $\boldsymbol{F}^e$ and a plastic part $\boldsymbol{F}^p$

$$\boldsymbol{F} = \boldsymbol{F}^e_M \boldsymbol{F}^p_M = \boldsymbol{F}^e_F \boldsymbol{F}^p_F \tag{2}$$

is assumed for the matrix, denoted with the index M, and for each fibre, denoted with the index F. The well known multiplicative decomposition implies a stress free intermediate configuration for the matrix and for each fibre. The time derivative of the deformation gradient reads

$$\dot{\boldsymbol{F}} = \boldsymbol{l}\boldsymbol{F} = \boldsymbol{F}\boldsymbol{L} \quad , \tag{3}$$

where $\boldsymbol{l}$ and $\boldsymbol{L}$ denote the left and the right rate. For the plastic deformation we define a right rate according to

$$\dot{\boldsymbol{F}}^p_M = \boldsymbol{F}^p_M \boldsymbol{L}^p_M \quad , \quad \dot{\boldsymbol{F}}^p_F = \boldsymbol{F}^p_F \boldsymbol{L}^p_F \quad . \tag{4}$$

The following quantities of the right Cauchy-Green type are defined by

$$\boldsymbol{C} = \boldsymbol{F}^T \boldsymbol{F} \quad , \quad \boldsymbol{C}^e_M = \boldsymbol{F}^{e\,T}_M \boldsymbol{F}^e_M \quad , \quad \boldsymbol{C}^p_M = \boldsymbol{F}^{p\,T}_M \boldsymbol{F}^p_M \quad . \tag{5}$$

For each fibre we introduce a structural tensor $\boldsymbol{M}_F := \boldsymbol{v}_F \otimes \boldsymbol{v}_F$, where the vector $\boldsymbol{v}_F$ is the normalized direction of the fibre. With the assumption that the plastic deformations of the fibre occur only in fibre direction

$$\boldsymbol{F}^p_F = \lambda^p \, \boldsymbol{M}_F \quad , \tag{6}$$

the right Cauchy-Green tensor reads

$$\boldsymbol{C} = \lambda^{p2} \boldsymbol{M}_F \boldsymbol{F}^{e\,T}_F \boldsymbol{F}^e_F \boldsymbol{M}_F \quad . \tag{7}$$

Therefore we define elastic and plastic right Cauchy-Green tenors of the fibre as

$$\boldsymbol{C}^e_F = \frac{1}{\lambda^{p2}} \boldsymbol{M}_F \boldsymbol{C} \boldsymbol{M}_F \quad , \quad \boldsymbol{C}^p_F = \lambda^{p2} \boldsymbol{M}_F \quad . \tag{8}$$

2.2. Free energy function and dissipation

The free energy function is introduced by

$$\Psi = \Psi_M(\boldsymbol{C}^e_M, Z_M) + \sum_{F=1}^{n_F} \Psi_F(\boldsymbol{C}^e_F, Z_F) \quad , \tag{9}$$

where n_F is the total number of fibres. The quantities Z_M, Z_F are the internal plastic variables for the matrix and a fibre. The localized form of the dissipation inequality for an isothermal process reads

$$\mathcal{D} = \boldsymbol{\Xi} : \boldsymbol{L} - \rho_{0\,M} \dot{\Psi}_M - \sum_{F=1}^{n_F} \rho_{0\,F} \dot{\Psi}_F \geq 0 \quad . \tag{10}$$

Here ρ_{0M} and ρ_{0F} are the densities of the matrix and fibre materials in the reference configuration and $\boldsymbol{\Xi}$ is the Mandel stress tensor, which is related to the Kirchhoff stress $\boldsymbol{\tau}$ and the 2^{nd}-Piola-Kirchhoff stress $\boldsymbol{S}$ by $\boldsymbol{\Xi} = \boldsymbol{F}^T\boldsymbol{\tau}\boldsymbol{F}^{-T} = \boldsymbol{C}\boldsymbol{S}$, see e.g. Sansour and Kollmann [17]. The rates of the free energy may be derived as follows:

$$\begin{aligned}\dot{\boldsymbol{C}}^e_M =& \boldsymbol{F}^p_M{}^{-T}\boldsymbol{L}^T\boldsymbol{C}\boldsymbol{F}^p_M{}^{-1} + \boldsymbol{F}^p_M{}^{-T}\boldsymbol{C}\boldsymbol{L}\boldsymbol{F}^p_M{}^{-1} \\ &- \boldsymbol{F}^p_M{}^{-T}\boldsymbol{L}^p_M{}^T\boldsymbol{C}\boldsymbol{F}^p_M{}^{-1} - \boldsymbol{F}^p_M{}^{-T}\boldsymbol{C}\boldsymbol{L}^p_M\boldsymbol{F}^p_M{}^{-1}\end{aligned} \tag{11}$$

and

$$\dot{\boldsymbol{C}}^e_F = \frac{1}{\lambda^p{}^2}\boldsymbol{M}_F\boldsymbol{L}^T\boldsymbol{C}\boldsymbol{M}_F + \frac{1}{\lambda^p{}^2}\boldsymbol{M}_F\boldsymbol{C}\boldsymbol{L}\boldsymbol{M}_F - 2\frac{\dot{\lambda}^p}{\lambda^p{}^2}\boldsymbol{M}_F\boldsymbol{C}\boldsymbol{M}_F \quad . \tag{12}$$

Considering the definitions

$$\boldsymbol{\Xi}_M := 2\,\rho_{0M}\,\boldsymbol{C}\boldsymbol{F}^p_M{}^{-1}\frac{\partial\Psi_M}{\partial\boldsymbol{C}^e_M}\boldsymbol{F}^p_M{}^{-T},\ \boldsymbol{\Xi}_F := 2\,\rho_{0F}\,\frac{1}{\lambda^p{}^2}\boldsymbol{C}\boldsymbol{M}_F\frac{\partial\Psi_F}{\partial\boldsymbol{C}^e_F}\boldsymbol{M}_F \tag{13}$$

$$Y_M := -\rho_{0M}\frac{\partial\Psi_M}{\partial Z_M} \qquad\qquad , \ Y_F := -\rho_{0F}\frac{\partial\Psi_F}{\partial Z_F} \tag{14}$$

in eq. (10) the dissipation inequality reduces to

$$\begin{aligned}\mathcal{D} =& (\,\boldsymbol{\Xi} - \boldsymbol{\Xi}_M - \sum_{F=1}^{n_F}\boldsymbol{\Xi}_F\,) : \boldsymbol{L} + \boldsymbol{\Xi}_M : \boldsymbol{L}^p_M + Y_M\,\dot{Z}_M \\ &+ \sum_{F=1}^{n_F}(\,\boldsymbol{\Xi}_F : \dot{\lambda}_p\,\boldsymbol{M}_F + Y_F\,\dot{Z}_F\,) \geq 0 \quad .\end{aligned} \tag{15}$$

Since inequality (15) must hold for arbitrary processes in the material, standard arguments in rational thermodynamics yield the equations

$$\boldsymbol{\Xi} = \boldsymbol{\Xi}_M + \sum_{F=1}^{n_F}\boldsymbol{\Xi}_F \tag{16}$$

$$\mathcal{D}_M = \boldsymbol{\Xi}_M : \boldsymbol{L}^p_M + Y_M\,\dot{Z}_M \geq 0 \tag{17}$$

$$\mathcal{D}_F = \boldsymbol{\Xi}_F : \dot{\lambda}^p\,\boldsymbol{M}_F + Y_F\,\dot{Z}_F \geq 0 \quad . \tag{18}$$

For the matrix material we assume isotropic behaviour. Therefore eq. (17) may be rewritten as $\mathcal{D}_M = -\boldsymbol{\tau}_M : \frac{1}{2}\mathcal{L}(\boldsymbol{b}^e)\boldsymbol{b}^e + Y_M\,\dot{Z}_M \geq 0$, where $\boldsymbol{b}^e_M$ is the elastic left Cauchy-Green tensor of

the matrix and $\mathcal{L}(\boldsymbol{b}_M^e)$ is the Lie time derivative. This equation is identical to the formulation in [15].

2.3. Elastic constitutive model

For the matrix material we follow the work of Simo [15] and assume that the elastic strain energy is a quadratic function of the logarithmic elastic principal stretches. The Youngs modulus and the Poisson ratio are denoted by E_M and ν_M, respectively.

To introduce the elastic constitutive model for the fibre, eq. (13) is rewritten as $\boldsymbol{S}_F = \boldsymbol{C}\boldsymbol{\Xi}_F = (2\rho_{0\,F}\,\dfrac{1}{\lambda^{p\,2}}\dfrac{\partial \Psi_F}{\partial \boldsymbol{C}_F^e} : \boldsymbol{M}_F)\;\boldsymbol{M}_F$. With the definition

$$\begin{aligned} \sigma_F &:= E_F\,\frac{1}{2} ln[tr(C_F^e)] \\ &= E_F\,\frac{1}{2}(ln[tr(\boldsymbol{M}_F\boldsymbol{C}\boldsymbol{M}_F)] - 2ln[\lambda^p]) \quad , \end{aligned} \tag{19}$$

where E_F denotes the Youngs modulus of a fibre, the 2^{nd}-Piola-Kirchhoff stress tensor reads

$$\boldsymbol{S}_F = \sigma_F \boldsymbol{M}_F \quad . \tag{20}$$

2.4. Plastic constitutive model

The plastic constitutive model is determined by the yield condition, which defines the elastic domain. For the matrix material we consider an isotropic yield criteria of the von Mises type

$$\begin{aligned} f_M &:= \sqrt{\frac{3}{2}\,\boldsymbol{\tau}_M^d : \boldsymbol{\tau}_M^d} - (Y_{M\,0} - Y_M) \leq 0 \\ Y_M &:= -h_M\,Z_M - (Y_{M\,\infty} - Y_{M\,0})(1 - exp[-\eta_M\,Y_M]) \quad . \end{aligned} \tag{21}$$

Here $\boldsymbol{\tau}_M^d$ means the deviatoric part of the Kirchhoff stress of the matrix and h_M, η_M, $Y_{M\,\infty}$, $Y_{M\,0}$ are plastic parameters. The evolution equations of the plastic variables are

$$\begin{aligned} \dot{\boldsymbol{C}}_M^p &= 2\,\hat{\gamma}\,\boldsymbol{C}^p(\boldsymbol{F}^{-1}\frac{\partial f_M}{\partial \boldsymbol{\tau}_M}\boldsymbol{F}) \\ \dot{Z}_M &= \hat{\gamma}\,\frac{\partial f_M}{\partial Y_M} \quad . \end{aligned} \tag{22}$$

where $\hat{\gamma}$ denotes the Lagrangian multiplier. For further details see [15], [18]. For the fibre we introduce the yield criterion

$$\begin{aligned} f_F &:= \sqrt{tr(\boldsymbol{M}_F \boldsymbol{\Xi}_F \boldsymbol{M}_F)^2} - (Y_{F0} - Y_F) \leq 0 \\ Y_F &:= -h_F \, Z_F - (Y_{F\infty} - Y_{F0})(1 - exp[-\eta_F \, Y_F]) \quad , \end{aligned} \tag{23}$$

with the plastic parameters h_F, η_F, $Y_{F\infty}$, Y_{F0}. The principle of the maximum plastic dissipation along with the fulfillment of the yield condition results in the optimization problem

$$-\mathcal{D}_F(\boldsymbol{\Xi}_F, Y_F) + \hat{\gamma} \, f_F(\boldsymbol{\Xi}_F, Y_F) \leq 0 \quad . \tag{24}$$

A partial derivation to the unknown variables $\boldsymbol{\Xi}_F$, Y_F yields the evolution equations

$$\begin{aligned} \dot{\lambda}^p \boldsymbol{M}_F &= \hat{\gamma} \, \frac{\partial f_F}{\partial \boldsymbol{\Xi}_F} \\ \dot{Z}_F &= \hat{\gamma} \, \frac{\partial f_F}{\partial Y_F} \quad , \end{aligned} \tag{25}$$

along with the loading and unloading conditions $f_F \leq 0$, $\hat{\gamma} \geq 0$ and $\hat{\gamma} f_F = 0$. Taking into account $\sqrt{tr(\boldsymbol{M}_F \boldsymbol{\Xi}_F \boldsymbol{M}_F)^2} = \sqrt{\sigma_F^2} \; tr(\boldsymbol{C} \boldsymbol{M}_F)$ one obtains the evolution equations as

$$\begin{aligned} \dot{\lambda}^p \boldsymbol{M}_F &= \hat{\gamma} \, sign(\sigma_F) \boldsymbol{M}_F \\ \dot{Z}_F &= \hat{\gamma} \quad . \end{aligned} \tag{26}$$

3. IMPLICIT INTEGRATION ALGORITHM

For the isotropic matrix material we apply an implicit exponential integration algorithm to integrate the plastic strains (22), see Simo [15]. The plastic parameter is defined by $\gamma = (t_{n+1} - t_n)\hat{\gamma}$, where $[t_{n+1}, t_n]$ is a typical time step. An implicit integration of the evolution

equations of the fibre (26) yields

$$\begin{aligned} \lambda^p_{n+1} &= \lambda^p_n + \gamma \; sign(\sigma_F) \\ Z_{F\,n+1} &= Z_{F\,n} + \gamma \quad . \end{aligned} \tag{27}$$

The unknown plastic parameter is iteratively determined by fulfillment of the yield condition (23) using a Newton iteration scheme ${f_F^{k+1}}_{n+1} = f^k_{F\,n+1} + \frac{\partial f^k_{F\,n+1}}{\partial \gamma}\Delta\gamma = 0$, where k denotes the iteration step. With

$$\begin{aligned} \frac{\partial f_{F\,n+1}}{\partial \gamma} =& \frac{\partial f_{F\,n+1}}{\partial \sigma_{F\,n+1}} \frac{\partial \sigma_{F\,n+1}}{\partial {\lambda^p}_{n+1}} \frac{\partial \lambda^p_{n+1}}{\partial \gamma} + \frac{\partial f_{F\,n+1}}{\partial Y_{F\,n+1}} \frac{\partial Y_{F\,n+1}}{\partial Z_{F\,n+1}} \frac{\partial Z_{F\,n+1}}{\partial \gamma} \\ =& - tr(\boldsymbol{C}_{n+1}\boldsymbol{M}_F)\frac{E_F}{\lambda^p_{n+1}} - (h_F + (Y_{F\infty} - Y_{F0})\,\eta_F\, exp[-\eta_F Z_{F\,n+1}]) \end{aligned} \tag{28}$$

the incremental update of $\gamma^{k+1} = \gamma^k + \Delta\gamma$ is given as

$$\Delta\gamma = -\frac{\sqrt{(\sigma^k_{n+1})^2}\, tr(\boldsymbol{C}^k_{n+1}\boldsymbol{M}_F) - (Y_{F0} - {Y_F}^k_{n+1})}{tr(\boldsymbol{C}^k_{n+1}\boldsymbol{M}_F)\,\frac{E_F}{{\lambda^p}^k_{n+1}} + (h_F + (Y_{F\infty} - Y_{F0})\,\eta_F\, exp[-\eta_F {Z_F}^k_{n+1}])} \quad . \tag{29}$$

3.1. Algorithmic consistent tangent modulus

The algorithmic consistent tangent tensor is defined by

$$\mathbb{C}_{n+1} := 2\frac{d\boldsymbol{S}_{n+1}}{d\boldsymbol{C}_{n+1}} \quad . \tag{30}$$

Considering the additive split of the stresses in eq. (16) one obtains

$$\begin{aligned} \mathbb{C}_{n+1} &= 2\frac{d\boldsymbol{S}_{M\,n+1}}{d\boldsymbol{C}_{n+1}} + \sum_{F=1}^{n_F} 2\frac{d\boldsymbol{S}_{F\,n+1}}{d\boldsymbol{C}_{n+1}} \\ &= \mathbb{C}_{M\,n+1} + \sum_{F=1}^{n_F} \mathbb{C}_{F\,n+1} \quad . \end{aligned} \tag{31}$$

The tangent of the isotropic matrix material is derived in [15]. For each fibre we take into account eq. (20) in which the structural tensor $\boldsymbol{M}_F$ is constant. The stress $\sigma_{F\,n+1}$ is a function of the right Cauchy-Green tensor $\boldsymbol{C}_{n+1}$ and the plastic parameter γ_{n+1}. The fulfillment of $f_{F\,n+1}(\sigma_{F\,n+1}, Y_{F\,n+1}) = 0$ implies that γ is a function of $\boldsymbol{C}$. Thus the derivation $\frac{d\sigma_{F\,n+1}}{d\boldsymbol{C}_{n+1}}$

reads

$$\frac{d\sigma_{F\,n+1}}{d\boldsymbol{C}_{n+1}} = \frac{\partial\sigma_{F\,n+1}}{\partial\boldsymbol{C}_{n+1}} + \frac{\partial\sigma_{F\,n+1}}{\partial\lambda^p_{n+1}}\frac{\partial\lambda^p_{n+1}}{\partial\gamma_{n+1}}\frac{\partial\gamma_{n+1}}{\partial\boldsymbol{C}_{n+1}} \quad . \tag{32}$$

Here the unknown $\dfrac{\partial\gamma_{n+1}}{\partial\boldsymbol{C}_{n+1}}$ may be derived by the use of the implicit derivation of $f_{F\,n+1}(\boldsymbol{C}_{n+1},\, \gamma_{n+1}(\boldsymbol{C}_{n+1}))=0$, which is

$$\begin{aligned}\frac{\partial f_{F\,n+1}}{\partial\boldsymbol{C}_{n+1}} + \frac{\partial f_{F\,n+1}}{\partial\sigma_{F\,n+1}}\Big(\frac{\partial\sigma_{F\,n+1}}{\partial\boldsymbol{C}_{n+1}} + \frac{\partial\sigma_{F\,n+1}}{\partial\lambda^p_{n+1}}\frac{\partial\lambda^p_{n+1}}{\partial\gamma_{n+1}}\frac{\partial\gamma_{n+1}}{\partial\boldsymbol{C}_{n+1}}\Big)\\ + \frac{\partial f_{F\,n+1}}{\partial Y_{F\,n+1}}\frac{\partial Y_{F\,n+1}}{\partial Z_{F\,n+1}}\frac{\partial Z_{F\,n+1}}{\partial\gamma_{n+1}}\frac{\partial\gamma_{n+1}}{\partial\boldsymbol{C}_{n+1}} = 0 \quad .\end{aligned} \tag{33}$$

With

$$\frac{\partial f_{F\,n+1}}{\partial\boldsymbol{C}_{n+1}} = \sqrt{(\sigma_{F\,n+1})^2}\;\boldsymbol{M}_F \quad , \frac{\partial f_{F\,n+1}}{\partial\sigma_{F\,n+1}} = sign(\sigma_{F\,n+1})\,tr(C_{F\,n+1}\boldsymbol{M}_F) \tag{34}$$

$$\frac{\partial\sigma_{F\,n+1}}{\partial\lambda^p_{n+1}} = -E_F/\lambda^p_{n+1} \qquad , \frac{\partial\lambda^p_{n+1}}{\partial\gamma_{n+1}} = sign(\sigma_{F\,n+1}) \tag{35}$$

$$\frac{\partial f_{F\,n+1}}{\partial Y_{F\,n+1}} = 1 \qquad , \frac{\partial Z_{F\,n+1}}{\partial\gamma_{n+1}} = 1 \tag{36}$$

it follows

$$\frac{\partial\gamma_{n+1}}{\partial\boldsymbol{C}_{n+1}} = \frac{1}{2}\,sign(\sigma_{F\,n+1})\,\frac{(2\sigma_{F\,n+1}+E_F)}{tr(\boldsymbol{C}_{F\,n+1}\boldsymbol{M}_F)\,E_F/\lambda^p_{n+1} - y_{F}{}'_{n+1}}\,\boldsymbol{M}_F \quad , \tag{37}$$

where $y_{F}{}'_{n+1}$ is defined as

$$y_{F}{}'_{n+1} := \frac{\partial Y_{F\,n+1}}{\partial Z_{F\,n+1}} = -(h_F + (Y_{F\infty} - Y_{F0})\,\eta_F\,exp[-\eta_F Z_{F\,n+1}]) \quad . \tag{38}$$

Inserting the latter equation and $\dfrac{\partial\sigma_{F\,n+1}}{\partial\boldsymbol{C}_{n+1}} = E_F/tr(\boldsymbol{C}_{F\,n+1}\boldsymbol{M}_F)$ in (32), the tangent modulus appears in the form

$$\mathbb{C}_{F\,n+1} = \Big(\frac{E_F}{tr(\boldsymbol{C}_{F\,n+1}\boldsymbol{M}_F)} - \frac{E_F(E_F+2\sigma_{F\,n+1})}{tr(\boldsymbol{C}_{F\,n+1}\boldsymbol{M}_F)\,E_F - y_{F}{}'_{n+1}\,\lambda^p_{n+1}}\Big)\boldsymbol{M}_F\otimes\boldsymbol{M}_F \quad . \tag{39}$$

4. NUMERICAL EXAMPLES

Some numerical examples demonstrate the main characteristics of the proposed model. Therefore the constitutive model is implemented into a 3D hexahedral element.

In the first example an element formulation is used, which is numerically integrated with one integration point and stabilized with the method proposed by Reese et al. [19]. For all other examples an element formulation suggested in [18] is considered. The following examples are calculated with an extended version of the program FEAP [20] and illustrate the anisotropic effects, which occur during large elastic-plastic deformations.

4.1. Necking of a specimen

In the first example the influence of the fibre direction θ on the overall behaviour of the structure is discussed. Therefore a necking problem of a specimen with a plane strain condition is investigated. The specimen, the geometrical data and the boundary conditions are shown in Figure 1. The nodal displacement u along the loaded edge is linked, a free contraction of the strip is allowed. The specimen is modelled with 60×20 elements in plane and one element through the thickness $t = 0.1$. The material data are summarized in Table I. Only one fibre is considered in this example.

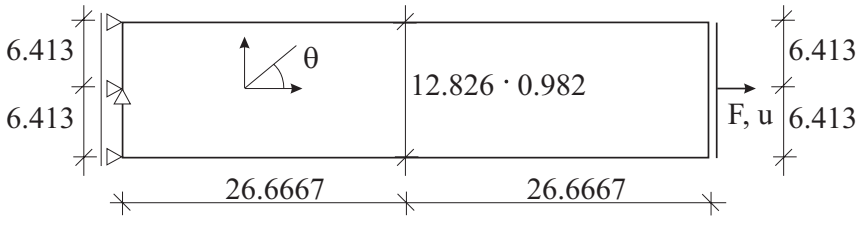

Figure 1. Geometry and boundary conditions of the specimen

With a displacement driven computation the specimen is stretched up to 22.5% in longitudinal direction. The deformed configurations with a plot of the equivalent plastic strains of the fibre and the matrix are shown in Figures 2, 3 for different fibre directions θ.

Table I. Material data for the matrix and the fibre

matrix	$E_M = 206.9,$	$\nu_M = 0.29,$		
	$Y_{M0} = 0.450,$	$Y_{M\infty} = 0.715,$	$h_M = 0.12924,$	$\eta_M = 16.930$
fibre	$E_F = 206.9,$			
	$Y_{F0} = 4.50,$	$Y_{F\infty} = 3.15,$	$h_F = 0.12924,$	$\eta_F = 16.930$

During the deformation the right edge of the specimen is moving upwards or downwards depending on the fibre direction. Furthermore Figures 2, 3 show, that the appearance of necking in the middle of the specimen is strongly influenced by the fibre direction.

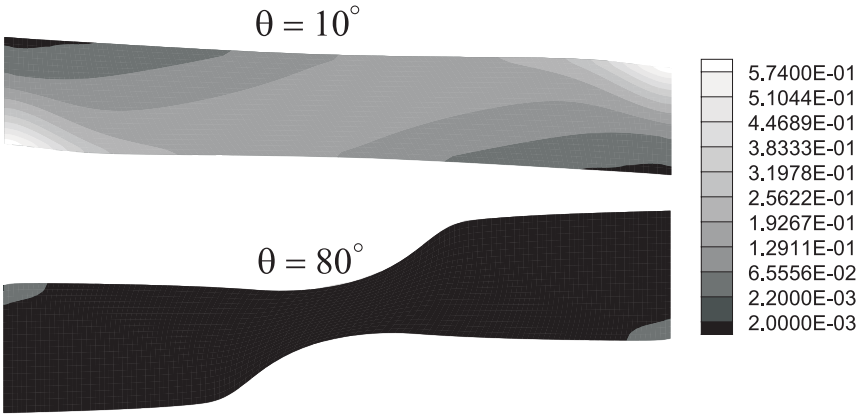

Figure 2. Equivalent plastic strains of the fibre

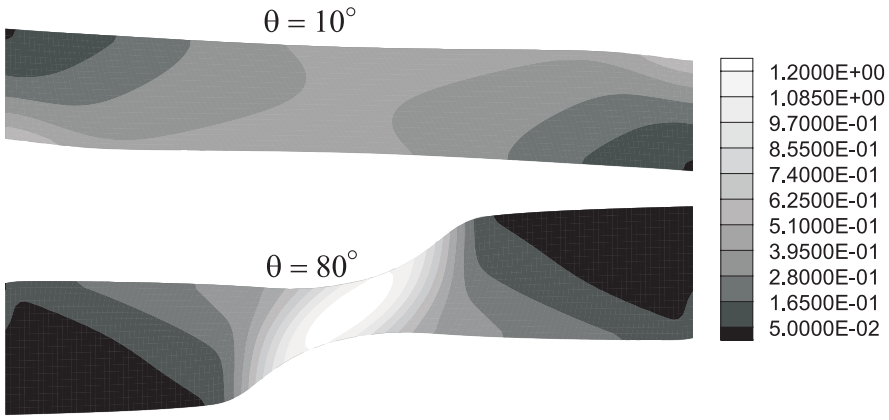

Figure 3. Equivalent plastic strains of the matrix

4.2. Circular blank

The next example, which was introduced in [8], demonstrates the difference between an elastoplastic fibre and an elastoplastic matrix.

A circular blank with a concentric circular hole is deep-drawn into a cup, see Figure 4. To simulate the drawing process without contact elements, the inner circular boundary is pulled uniformly inwards in a radial direction up to a maximum displacement of 120, while the outer edge is free. A plane strain condition is considered for the calculation. The circular blank is modelled with 10×40 elements in plane and one element through the thickness.

For the material behaviour it is distinguished between an elastic matrix with an elastic-plastic fibre material and an elastic-plastic matrix with an elastic fibre material. The yield stress either for the fibre or for the matrix is given by 0.45. No hardening is assumed for the plastic behaviour. The Youngs-moduli of the fibre and the matrix are identical. Two fibres with the fibre directions of $\Theta = \pm 45^0$ degree are assumed.

In Figure 5 the deformed configurations with the equivalent plastic strains of the fibres are

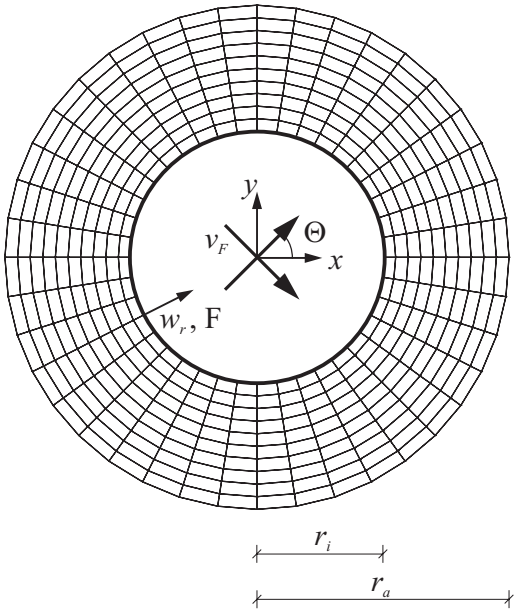

geometry:	r_i	=	200
	r_a	=	400
	t	=	10
matrix:	E_M	=	206.9
	ν_M	=	0.29
	Y_{M0}	=	0.450
fibre:	E_F	=	E_M
	Y_{F0}	=	0.450

Figure 4. Geometry of the circular blank and its material data

depicted, the matrix material is assumed to be elastic. Whereas in Figure 6 the deformed configurations with the equivalent plastic strains of the matrix are shown and the fibre is assumed to be elastic.

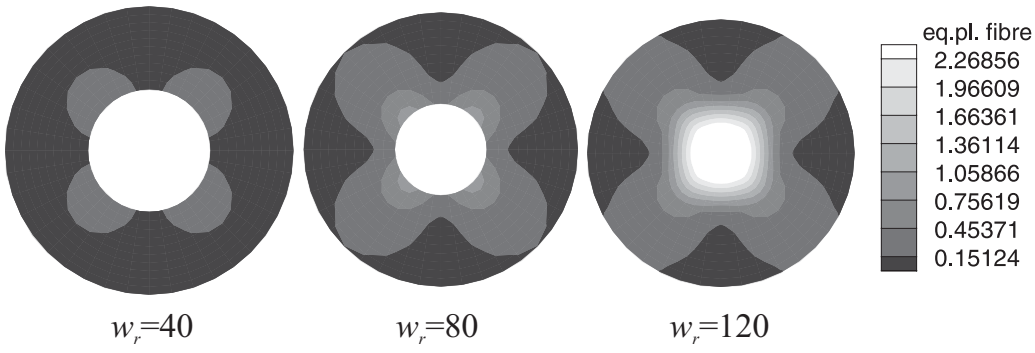

Figure 5. Deformed configurations with a plot of the equivalent plastic strains of the fibre

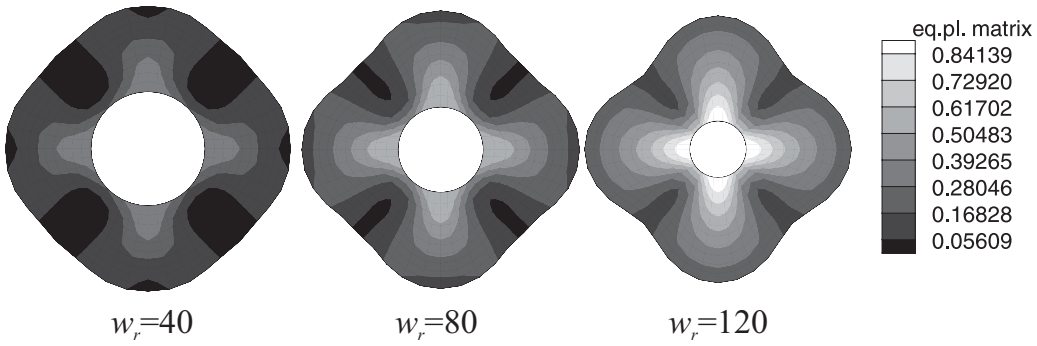

Figure 6. Deformed configurations with a plot of the equivalent plastic strains of the matrix

The equivalent plastic strains of the fibre occur mainly in the fibre direction under the angle of $\Theta = \pm 45^0$ degree. In opposite to that, the plastic strains of the matrix arise mainly along the x and y directions. Here, the deformed structure is characterized by the so called 'earing' which occurs at the free edge. The same characteristic was obtained in [8], [12], where an anisotropic yield function has been used.

4.3. Punching of a conical shell

The last example demonstrates the strong anisotropic response of a structure due to the presence of fibres. A conical shell is loaded eccentrically at the upper outer rim and supported at the lower outer rim. For the geometry data and the material parameters see Figure 7. One quarter of the shell structure is discretized with 8×8 elements and one element through the thickness.

For the fibre material it is distinguished between a stiff and a soft material set. The fibre direction is indicated with the arrows shown in Figure 7 and is supposed to be constant for each quarter of the shell. Only linear hardening is taken into account for the matrix and the fibre material. The non-linear behaviour is computed using an arclength method with displacement

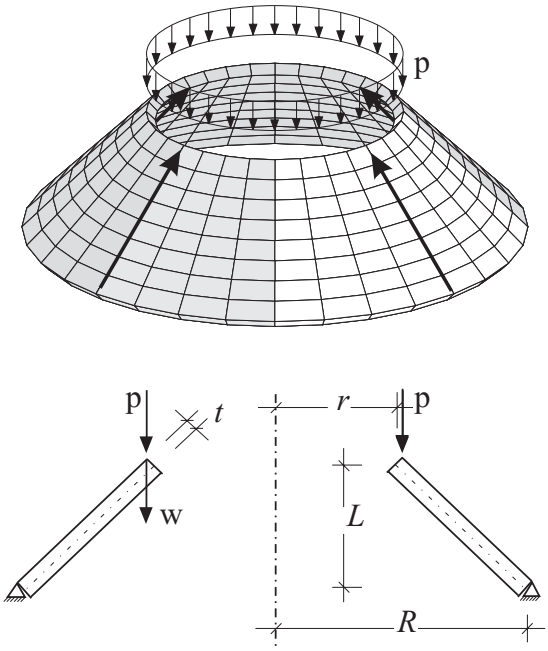

fibre:

	stiff model	soft model
E_F =	1241.40	310.35
Y_{F0} =	2.70	0.450
h_F =	0.414	0.414

matrix: $E_M = 206.9$

$\nu_M = 0.29$

$Y_{M0} = 0.450$

$h_M = 0.4138$

geometry: $r = 2.70$

$R = 0.414$

$L = 1$

$t = 0.1$

Figure 7. The geometry of the conical shell and its material data

control, which leads to the load deflection curve shown in Figure 8.

In the diagram the load p is plotted over the vertical displacement w of the upper rim of the conical shell for different material sets. The isotropic model consists out of the matrix material without any fibre and is denoted by the solid line. The fibre-matrix material with the soft fibres, which is denoted by the line with circles, shows almost the same characteristic through

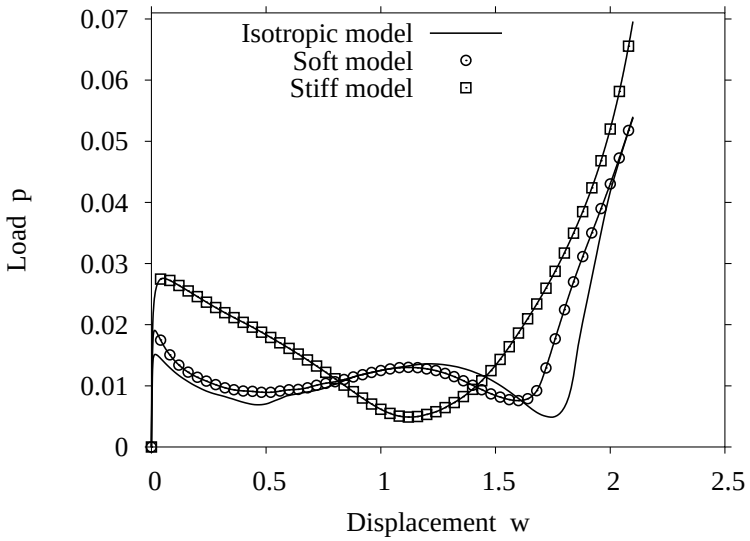

Figure 8. Load deflection curve of the conical shell

the hole loading process as the isotropic material.

The load is increased until the elastic limit load is reached at w≈ 0.04. Hence a rolling process starts at the top of the shell until a second stability point at w≈ 0.5 is traced. Here a global snap through behaviour of the shell is observed. At the local minimum w≈ 1.6 the stable path is reached and the load is increased until w= 2.1.

The stiff model, displayed by the line with squares, leads to a complete different characteristic of the load deflection curve. Here the local minimum at $w \approx 0.5$ is not reached, which means that the rolling up and the snap through phenomena arise in one step.

The deformed meshes with a plot of the equivalent plastic strains are shown in Figures 9, 10 at characteristic points for the stiff fibre-matrix model. Here, the first plastic strains emerge when the elastic limit load is reached. At this point one obtains that the rolling up process starts form the upper edge. Obviously the deformed structure at w= 0.5 is wavily and the distributions of the equivalent plastic strains for the fibre as well as for the matrix are not

rotationally symmetric. At w= 1.21 until w= 1.6 the snap through phenomenon is dominating the structural behaviour. The equivalent plastic strains attain a maximum at w= 2.1. The maximum of the equivalent plastic strain of the matrix is 143% and the plastic strain of the fibres increases to a maximum of 6%. The stiff fibre matrix model shows strong anisotropic effects through the hole loading process.

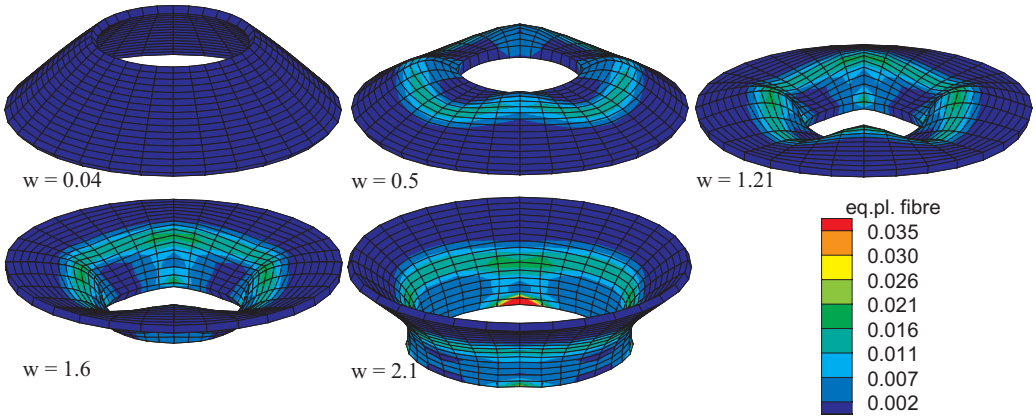

Figure 9. Deformed configurations with a plot of the equivalent plastic strains of the fibre for the stiff fibre-matrix material model

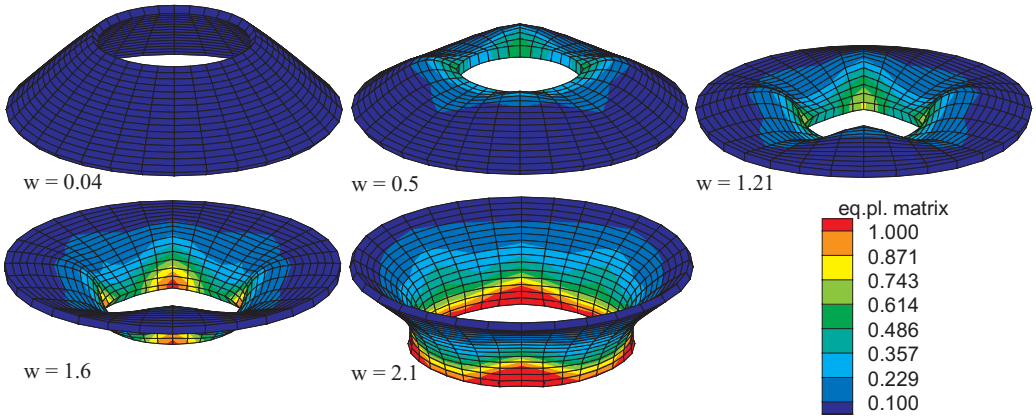

Figure 10. Deformed configurations with a plot of the equivalent plastic strains of the matrix for the stiff fibre-matrix material model

5. CONCLUSION

In this paper a computational framework for the analysis of fibre reinforced materials at finite elastic-plastic deformations is presented. A constitutive model for anisotropic finite strain plasticity was introduced. The additive split of the free energy function leads to separated constitutive equations for the matrix and for the fibres. The material behaviour of the matrix is assumed to be isotropic. The anisotropic effect is induced by the fibres, which are described by macroscopic one-dimensional material models. The governing equations were derived with the principle of maximum dissipation along with the yield condition as a constraint. A set of numerical examples demonstrated the numerical efficiency of the whole approach.

REFERENCES

1. Boehler JP. Introduction to the invariant formulation of anisotropic constitutive equations. In *Application of Tensor Functions in Solid Mechanics,* Boehler JP (eds). CISM Courses and Lectures No. 292. Springer: Wien/New York, 1987; 13–64. 1
2. Dvorak GJ, Bahei-El-Din YA, Macheret Y, Liu CH. An experimentalstudy of elastic-plastic behavior of a fibrous boron-aluminum composite. *J. Mech. Phys. Solids* 1988; **36**:665–687. 1
3. Spencer AJM. Plasticity theory for fibre-reinforced composites. *J. Eng. Math.* 1992; **26**:107–118. 1
4. Hill R. *The Mathematical Theory of Plasticity.* Clarendon Press: Oxford, 1950. 1
5. Spencer AJM. Anisotropic invariants and additional results for invariant and tensor representations. In *Application of Tensor Functions in Solid Mechanics,* Boehler JP (eds). CISM Courses and Lectures No. 292. Springer: Wien/New York, 1987; 171–186. 1
6. Oller S, Car E, Lubliner J. Definition of a general implicit orthotropic yield criterion. *Comput. Meth. Appl. Mech. Eng.* 2003; **192**:895–912. 1
7. Rogers TG. Yield criteria, flow rules, and hardening in anisotropic plasticity. In *Yielding, Damage, and Failure of Anisotropic Solids,* Boehler JP (eds). EGF5, Mechanical Engineering Publications: London, 1990. 1

8. Papadopoulos P, Lu J. On the fomulation and numerical solution of problems in anisotropic finite plasticity. *Comput. Meth. Appl. Mech. Eng.* 2001; **190**:4889–4910. 1, 4.2, 4.2
9. Schröder J, Gruttmann F, Löblein J. A simple orthotropic finite elasto-plasticity model based on generalized stress-strain measures. *Comp. Mech.* 2002; **30**:48–64. 1
10. Apel N, Miehe C. Anisotropic finite plasticity in the logarithmic strain space. a modular formulation based on a " small-strain box " of incremental variational updates. In *Fifth Wolrd Congress on Computational Mechanics,* Mang HA, Rammerstorfer FG, Eberhardsteiner J (eds). WCCM V: Vienna, Austria, 2002. 1
11. Sansour C, Bocko J. On the numerical implications of multiplicative inelasticity with an anisotropic elastic constitutive law. Int. J. Num. Meth. Eng. 2003; **58**:2131–2160. 1
12. Gruttmann F, Eidel B. On the implementation of anisotropic finite strain plasticity. In *Fifth Wolrd Congress on Computational Mechanics,* Mang HA, Rammerstorfer FG, Eberhardsteiner J (eds). WCCM V: Vienna, Austria, 2002. 1, 4.2
13. Menzel A, Steinmann P. On the spatial formulation of anisotropic multiplicative elasto-plasticity. *Comput. Meth. Appl. Mech. Eng.* 2003; **192**:3431–3470. 1
14. Reese S. Meso-macro modelling of fibre-reinforced rubber-like composites exhibiting large elastoplastic deformations. *Int. J. of Sol. and Struc.* 2003; **40**:951–980. 1
15. Simo JC. Algorithms for static and dynamic multiplicative plasticity that preserve the classical return mapping schemes of the infinitesimal theory. *Comput. Meth. Appl. Mech. Eng.* 1992; **99**:61–112. 1, 2.2, 2.3, 2.4, 3, 3.1
16. Simo JC, Hughes TJR. *Computational Inelasticity. Mechanics and Materials.* vol. 7. Springer: New York, 1998. 1
17. Sansour C, Kollmann FG. Large viscoplastic deformations of shells. Theory and finite element formulation. *Comp. Mech.* 1998; **21**:512–525. 2.2
18. Wagner W, Klinkel S, Gruttmann F. Elastic and plastic analysis of thin-walled structures using improved hexahedral elements. *Comput. & Struct.* 2002; **80**:857–869. 2.4, 4
19. Reese S, Wriggers P. A stabilization technique to avoid hourglasing in finite elasticity. *Int. J. Num. Meth. Eng.* 2000, **48**:79–109. 4
20. Taylor RL. Feap - manual. http:\\www.ce.berkeley \ ∼ rlt \ feap \ manual.pdf [November 2003]. 4